Available online at www.sciencedirect.com

ScienceDirect

journal homepage: www.elsevier.com/locate/issn/15375110

Research Paper

Micro-CT imaging of tomato seeds: Predictive potential of 3D morphometry on germination

Laura Gargiulo [a], Cristina Leonarduzzi [b], Giacomo Mele [a,*]

[a] Institute for Agricultural and Forest Systems in the Mediterranean (ISAFoM), Department of Biology, Agriculture and Food Sciences (DiSBA), National Research Council (CNR), Italy
[b] Seed Technology Department, ISI Sementi S.p.a, Italy

ARTICLE INFO

Article history:
Received 7 June 2020
Received in revised form
9 August 2020
Accepted 11 September 2020

Keywords:
Seedlings
Discriminant analysis
Seed morphological traits
X-ray exposure effect
Seed phenotyping

The relationship between seed physical characteristics and seed quality is widely investigated by using X-ray based imaging techniques. Recently the use of X-ray micro-tomography (micro-CT) is increasingly used for more accurate characterisation of the internal seed morphology. In this work a germination test was carried out along with the morphometric characterisation of tomato seed internal structure by means of X-ray micro-CT and 3D image analysis. The aim was to accurately evaluate the predictive potential of internal seed 3D morphology for germination outcomes. The visual assessment allowed the relationship between specific internal seed abnormalities and the different germination outcomes to be demonstrated experimentally. Univariate analysis of morphometric seed traits allowed 3D free space % and Sauter diameter, among the most discriminant parameters, to be identified as the most effective for the prediction of germination outcomes. Discriminant Analysis (DA) of 3D morphometric dataset correctly classified 96.3% of normal seedlings, 83.3% of ungerminated seeds and 63.6% of abnormal seedlings, providing a high overall prediction potential of 91.9%. The above analyses have also been performed referring to the germination at 5 days after sowing. As a side effect of the applied technique, an increase of abnormal seedlings was observed at increasing X-ray exposure level.

Overall, X-ray micro-CT coupled with DA of internal morphometric traits has proved to be an effective tool to investigate the relationship between tomato seed 3D morphology and seed physiology, although attention has to be paid to possible consequences of X-ray exposure.

1. Introduction

Seed quality research aims to enhance the uniformity of development, yield and quality of the harvested product. This, in turn, makes possible increased profit for both farmers and seed dealers (Xia et al., 2019).

Identifying predictive morphological traits of seed quality and their germination has long been addressed using conventional radiography as a technique to observe internal seed structures and to guide seed sorting (e.g., van der Burg et al., 1994), as well as to monitor seed maturation (e.g., Downie et al., 1999).

* Corresponding author.
E-mail address: giacomo.mele@cnr.it (G. Mele).
https://doi.org/10.1016/j.biosystemseng.2020.09.003

De Medeiros et al. (2020) studied pepper seed maturation by means of radiographic images and observed that the relative density (i.e. the mean of the gray values of all the pixels in the selected area) may be an indication of the degree of seed maturation. Gagliardi and Marcos-Filho (2011) and Dell'Aquila (2007) also related high tissue density to the germination performance of pepper seeds.

Many studies based on X-ray radiography have been carried out also for tomato seeds, and identified that besides the percentage of internal free space, abnormalities of embryo or internal tissue defects have to be addressed to predict germination behaviour (Borges et al., 2019; Downie et al., 1999; Silva et al., 2013; van der Burg et al., 1994). In particular, internal morphological traits affect germination depending on their extent and localisation (Silva et al., 2013), and their detection is not always possible by means of conventional radiography (Gomes & van Duijn, 2017). Moreover, X-ray radiography also presents some limitations in internal inspection for large seed size and usefulness only for flat seeds (Gomes & van Duijn, 2017).

Three-dimensional X-ray imaging in seed science research and technology has become increasingly common. X-ray micro-tomography allows an accurate visualisation of the internal seed parts and, for example, the identification of micro cracks not observable by conventional X-ray radiography (Gomes & van Duijn, 2017). Indeed, 3D X-ray imaging has been recognised as a potential tool for the classification of seeds based on the characterisation of internal morphology (Xia et al., 2019), as it was shown for muskmelon and maize seed structure studied in relation to germination (Ahmed et al., 2018; Gomes-Junior et al., 2019). Arkhipov et al. (2019) observed that the method of computer microtomography can be recommended, taking into account the factors that limit its wide application in seed science (time expenditure on research and cost of equipment), for solving fundamental problems of seed science including control of the results of the breeding process because of its informativeness. Moreover, as stated by the International Seed Testing Association (ISTA) (Gomes & van Duijn, 2017), X-ray micro-CT is expected to be part of standardised seed tests. Indeed, a testing system based on X-ray microtomography has recently been provided by Porsch (2020) for sugar beet seeds.

On the other hand, it is necessary to consider and investigate in more depth the possible effect of the use of X-ray radiation both on seed germination and the seedling. Experiments involving X-ray irradiation, conducted on different seeds (e.g., Bino et al., 1993; Gomes-Junior et al., 2019), have shown that dose absorption can change with different source setups and, consequently, can produce different effects on germination outcomes (e.g., Rezk et al., 2019).

To the best of our knowledge, 3D X-ray imaging has never been used to quantitatively characterise internal structure of tomato seeds. In this framework, the aim of this study was to use X-ray micro-CT imaging to accurately explore the predictive potential of morphology of tomato seeds on germination outcomes. A sample of 105 seeds was scanned using an X-ray microtomograph and the internal and external morphological seed traits were qualitatively and quantitatively determined in three dimensions. Subsequently a germination test was carried out on the same seeds whose identity remained traced during the whole investigation. A side experiment was also performed with four different X-ray exposure levels, in order to evaluate the X-ray exposure effects on seed germination due to the micro-CT scans.

2. Material and methods

2.1. Plant material and germination tests

Seeds from a specific lot of a tomato variety developed by ISI Sementi S.p.a, have been used for this study. The initial storage conditions were 15 °C and 35% RH. They then underwent a regular two-step disinfection procedure using first calcium hypochlorite $Ca(ClO)_2$ solution, then trisodium phosphate Na_3PO_4 solution to remove fungi and bacteria from the seed surface, and finally were carefully rinsed with water. After oven-drying at 30 °C for 6 h, seeds where cleaned using a brushing machine and sieved to create a uniform seed lot. After these processing steps, seeds were stored and conserved in a conditioned room again at 15 °C, 35% RH.

From this seed lot, a sample of 105 seeds was randomly extracted to perform the morphological characterisation of each individual, whose identity was retained throughout the study. These seeds were individually weighed using an electronic analytical balance (Sartorius A200S: 0.001 g resolution). Additionally, from the cleaned seed lot, another three samples of 100 seeds each were randomly extracted in order to evaluate the effect of X-ray exposure on germination outcome.

Germination tests following ISTA protocol (ISTA, 2019) were carried out for all four seed samples. Seeds were sown in Petri dishes on water imbibed paper and then placed in a germination chamber for 16 h at 30 °C/8 h at 20 °C in a light/dark daily cycle. Two counts were performed: the first 5 days after sowing and the other after 14 days. The first count indicated germination speed, whereas the final count allowed a proper evaluation of the germination outcome and thus the potential to obtain normal plants. At the second count (14 d), normal seedlings were distinguished from abnormal seedlings, and dead seedlings from ungerminated seeds. It should be noted that in this work, differently from the definition reported in the ISTA rules (International Seed Testing Association, 2019), dead seeds were defined as germinated seeds that die a few days after germination. In the following, "normal", "abnormal", "dead" and "ungerminated" refer to both the corresponding germination outcomes and to the seeds that produced that outcome. In Fig. 1, example pictures of these germination outcomes are reported.

2.2. X-ray microCT

The X-ray microCT scans were performed using a desktop microtomograph (Bruker Skyscan 1272; http://bruker-microct.com/products/1272.htm). It is equipped with a cone beam X-ray source adjustable in the 20–100 kV energy range, which allows a cylinder-shaped volume of 6.5 cm in diameter and 7.2 cm height as maximum sample size. Eighteen seeds at a

time were scanned by arranging them in two superimposed circles, fitted on the curved surface of a polystyrene cylinder of 1.5 cm diameter, 1 cm height. Polystyrene was chosen for the cylinder because of its low X-ray attenuation capacity, allowing good contrast in the imaging of the seeds. The seed arrangement around the cylinder surface allowed a 3D image to be obtained in which seeds did not touch each other, simplifying the following stage of image processing and helping to maintain the individual seed identity. Six polystyrene sample holders were used to scan each seed sample by six image acquisitions. In order to obtain 3D images of the internal structure of the seeds, voltage and current of the X-ray source were set at 50 kV and 200 μA, respectively, according to the protocol defined by Gargiulo et al. (2019) for quinoa grains, which have similar size to tomato seeds. The distance between the cylinder and the X-ray source was 75 mm. About 900 X-ray projection images, one for each 0.2 degrees of sample rotation, were acquired in approximately 54 min at a resolution of 6.5 μm voxel size.

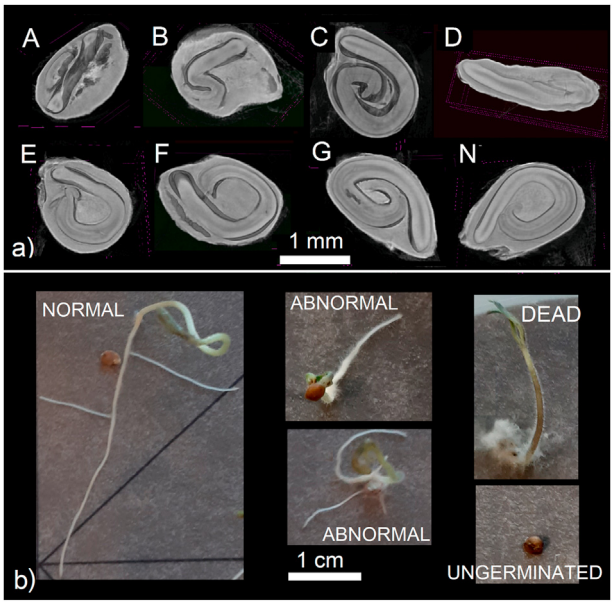

Fig. 1 – a) Examples of sections of three-dimensional reconstructions of tomato seeds with different internal morphological traits: A) strongly deformed embryo, B) slightly deformed embryo, C) strongly reduced endosperm, D) sideways curved cotyledons, i.e. oriented perpendicular to the transverse plane of the seed, E) reflexed cotyledons, i.e. one or both cotyledons sharply reflexed inside the seed, F) holes in the endosperm, G) fractures in the cotyledon(s), N) normal seed structure. b) Examples of germination test outcomes: normal seedling, abnormal seedling, dead seed, ungerminated seed.

2.3. Evaluation of X-ray exposure effects

Four levels of X-ray exposure have been considered in this experiment. One level was the control test with no X-ray exposure. One was the level used for morphological characterisation of the seeds. Other two levels were one higher and the other lower than that used for the morphological characterisation, thus simulating two other microtomographic scanning setups.

The levels of exposure were measured through an index of exposure to X-rays proportional to the source energy and exposure time and inversely proportional to the distance of the seed sample from the X-ray source according to the following formula:

$$\textit{Index of Xray radiation exposure} = \frac{\textit{source voltage}(kV)*\textit{exposure time}(min)}{\textit{distance between sample and Xray source}(mm)}$$

Then a "relative index" of the X-ray radiation was calculated for each exposure level by dividing the above index by the value obtained at the maximum level. In Table 2 the four scanning setups of the microtomograph and the corresponding radiation exposure levels are reported.

After the X-ray exposure, the results of the germination test were collected and analysed considering four 25 seeds subsamples for each exposure level.

2.4. Three-dimensional seed morphology characterisation

2.4.1. Image processing

The series of two-dimensional X-ray projection images obtained from each micro-CT scan were used to reconstruct 3D images using the NRecon software, version 1.7.3 (www.bruker-microct.com). The reconstruction procedure comprised a filtered back projection algorithm (Xiao et al., 2003). In order to obtain a proper 3D reconstruction of the images, ring artefact and beam hardening corrections were applied at 10% and 30% levels, respectively. The reconstruction time, for each eighteen seeds group, was 14 min. Then regions of interest (ROIs), each a parallelepiped including one seed at a time, were isolated from the reconstructed 3D images in order to characterise, both qualitatively and quantitatively, internal and external morphology of each single seed. DataViewer software, version 1.5.6.2 (www.bruker-microct.com), was used for selecting the ROIs.

2.4.2. Qualitative seed morphology

Visual observation of the internal structure of each seed was performed using CTvox sofware version 3.3.0 (www.bruker-microct.com). It allowed seed damages or abnormalities regarding the seed components to be recognised. Then, based mostly on descriptions found in the literature (Silva et al., 2013; van der Burg et al., 1994), the internal morphological traits defined in the caption of Fig. 1 were identified and scored for all the 105 seeds. Figure 1 shows an example of each scored seed morphological trait.

Table 1 – List of parameters used for morphological quantification of tomato seeds.

Free space %	Volume of the internal free space reported as percentage of the total volume of the seed
Sauter diameter	Diameter of a sphere with a ratio between volume and surface area equal to that measured for the seed
Solid phase volume	Volume of the seed solid phase
Structure thickness	Average thickness of the solid phase of the seeds
Seed surface	Sum of the internal and external surface areas of the seed
Equivalent rod length	Length of a shaft of homogeneous mass with central moment of inertia equivalent to that of the seed
Structure model index	The structure model index (SMI) is a parameter intended for determining the plate- or rod-like geometry of trabecular structures (Hildebrand & Rüegsegger, 1997). Indicative of the type of connectivity between the solid parts inside the seed
Major diameter	Maximum diameter of the seed
Total volume	Volume of the whole seed
Volume-equivalent sphere diameter	Diameter of a sphere with volume equal to that of the seed
Sphericity	Measurement of the proximity of the seed shape to spherical shape (value 1 in case of coincidence with the sphere)
Surface-equivalent sphere diameter	Diameter of a sphere with surface area equal to that of the seed
Surface convexity index	Indicative of the ratio between the area of the convex and concave surfaces present in the seed

Table 2 – Scanning setups to test impact of X-ray radiation exposure on tomato seed germination.

Level	kV	t (min)	dist (mm)	Index of X-ray radiation exposure	Relative index of X-ray radiation
0	0	0	0	0	0
1	50	34	93	18.3	0.25
2	50	54	75	36	0.50
3	50	135	93	72.6	1

2.4.3. *Quantitative seed morphology*

Quantification of volumetric and morphological traits was performed on the reconstructed images by applying the so-called "Object-based Image Analysis" approach (e.g., Blaschke, 2010). The 3D ROIs around all seeds were binarised applying a manual threshold to the grey level histograms in order to segment the solid phase of each seed. The segmented images were used to obtain morphometric parameters describing the whole seed, considering also the presence of the internal free space. This approach was applied using the CTan software, version 1.18.8 (www.bruker-microct.com). In particular, total volume, solid phase volume, percent free space, seed surface, structure model index, structure thickness, equivalent rod length, major diameter, volume-equivalent sphere diameter, surface-equivalent sphere diameter, Sauter diameter, sphericity and surface convexity index were determined for each seed (Table 1).

2.5. *Statistical analysis*

ANOVA and Tukey tests at $p < 0.05$ significance have been performed for each morphometric parameter to determine significant differences among the germination results. Linear regressions between germination results and X-ray exposure levels were determined. Pearson correlation coefficients between all combination of pairs of morphometric parameters were calculated determining also the corresponding p-values. Discriminant analysis (DA) was performed between germination results and non-autocorrelated morphometric parameters. DA was carried out twice using both assumptions, common and separate within-group covariance matrices, which produce linear and quadratic decision boundaries of group-membership, respectively (Tharwat, 2016). Except for DA, which was carried out using SPSS software version 26.0 (www.ibm.com), all statistical analyses were performed using Sigmaplot software, version 13.0 (www.systatsoftware.com).

3. Results and discussion

3.1. *X-ray exposure effects*

The germination outcomes after 14 days and the first count of germinated seeds after 5 days from the beginning of the germination are reported (Fig. 2) as ratio of the number of seeds with a given outcome to the total number of seeds. Measured values are reported for each relative index of X-ray radiation together with linear regression fits. In the Supplementary Material S1, all used data and linear regression parameters are reported. A good linear fit ($R^2 = 0.90$) and a significant increasing trend with the X-ray exposure were found for the abnormal seedling outcome, while negligible and not significant changes were found for dead and ungerminated seeds, as well as for the first count of germinated seeds after five days.

Our findings demonstrate that X-ray effects on tomato seeds are evident on 14 days old seedlings, in agreement with Dhamgaye et al. (2018), who observed that the effect of seed irradiation on growth of the bean seedlings depends upon the growth status. In particular, we have found that, for tomato seeds, X-rays did not affect the total count of germinated seeds but did affect abnormalities of the seedlings (see examples in Fig. 1). Different results have been found by Gomes et al. (2019), who used high-energy X-ray doses (89 keV) and did not observed negative effects on maize seed germination. Thus, when performing X-ray microtomography of tomato

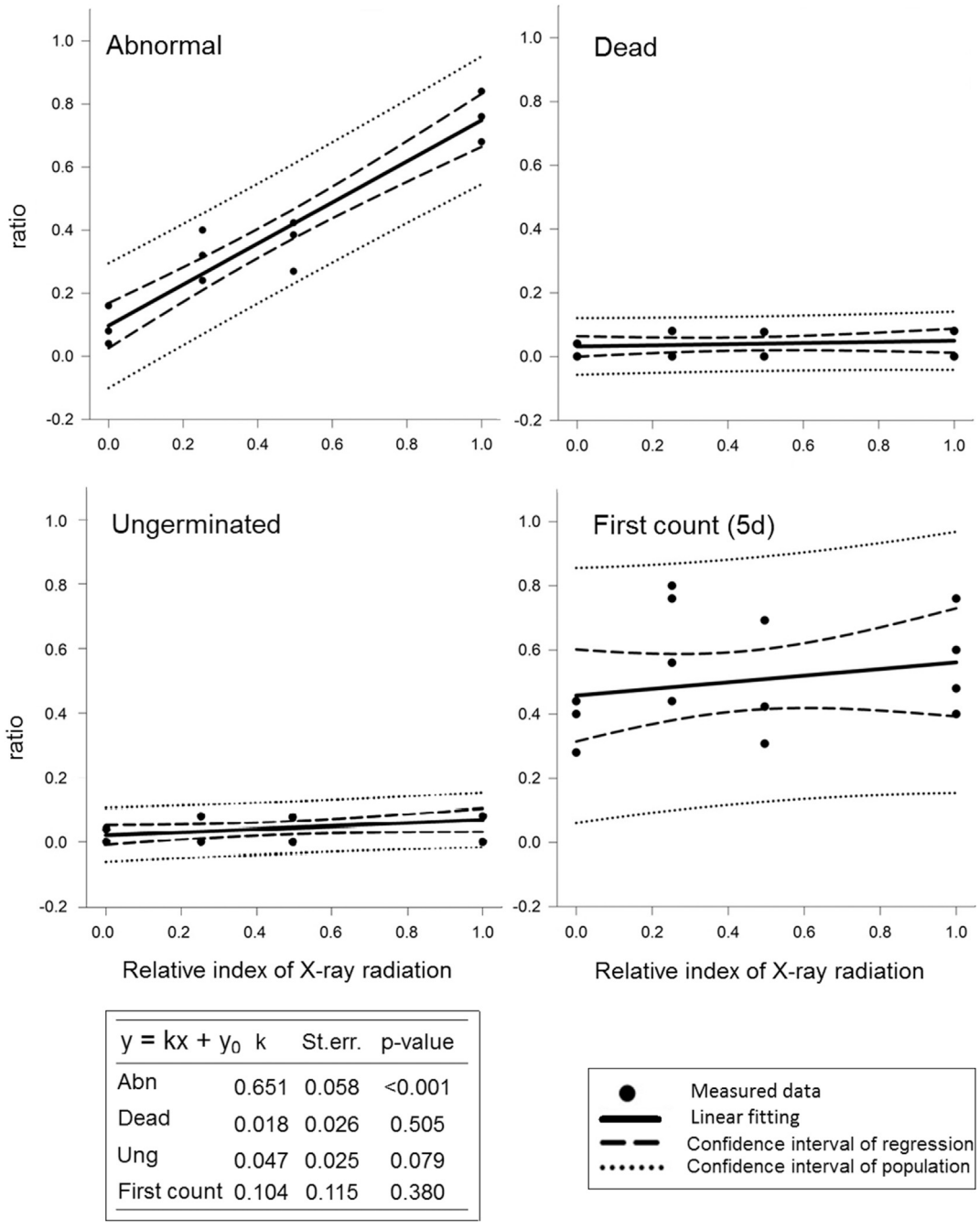

Fig. 2 – Linear regressions of the first count, abnormal, dead or ungerminated outcome as a function of the relative index of X-ray radiation. The ordinate axis indicates the ratio between the number of seeds with a given outcome and the total number of sample seeds. In the box are the slope parameters of the linear regressions coupled with standard errors and p-values (statistical significance $\alpha = 0.05$).

seeds, it is advisable to search for the optimal scanning setup in order to limit x-ray exposure while providing a good imaging result. In particular, in addition to minimising the X-ray source power and exposure time, we chose the size of the sample holder in a way that all the seeds were included in a single field of view of the detector, thus avoiding offset and oversize scanning modes, which give further exposure for the seeds temporarily out of the field of view.

3.2. *Prediction potential of seed morphology*

In order to properly explore the predictive potential of three-dimensional morphology for germination of tomato seeds, we firstly evaluated the frequency of a given germination outcome for each qualitative seed trait defined in Fig. 1a. Then, quantitative information has been used with both univariate and multivariate approaches. The univariate analysis

sought to identify the morphological parameters whose mean value better allowed germination outcomes to be differentiated. For the multivariate analysis, the discriminant analysis was performed as a probabilistic classifier. In the following analysis, the bias due to the X-ray exposure effects on the germination outcomes was also taken into account when classifying the abnormal germination outcome as described in Appendix A.

3.2.1. *Qualitative morphology*

The qualitative analysis of seed morphology consisted of visual assessment of the 3D internal structure of each seed, in order to determine the presence of one or more of the morphological traits described in the caption of Fig. 1a.

In Table 3 the numbers and the percentages of the seeds with a given morphological trait are shown in order to evaluate the relationship between germination outcomes and the observed morphological traits.

It can be noted that the alphabetical order of morphological traits in Table 3 correspond to an increasing percentage of normal germination outcome, except for an inversion between G and N traits. In particular, the presence of A and B traits (i.e., different levels of embryo deformation) determined only negative germination outcomes (i.e., abnormal, dead or ungerminated). Furthermore, trait A (strongly deformed embryo) was found only in dead or ungerminated seeds.

The alphabetical order of the morphological traits corresponds overall to a decreasing trend of negative effects on germination. In other words, our experimental results confirm that the most critical morphological traits are abnormalities of the whole embryo, followed by those of the endosperm, then those of cotyledons and finally damage to endosperm or cotyledons. Such a finding agrees with Silva et al. (2013), who stated that structural damage affected germination depending on its extent and localisation, but our approach allowed more precise identification of such a dependence.

Van der Burg et al. (1994) described as morphologically abnormal all the seeds we distinguished with different traits from A to E, and they then checked for correspondence with germination. Our approach allowed the relationship of each single trait with germination outcome to be better specified. For example, van der Burg stated that the amount of endosperm is critical for normal seedling development, while our results (see Table 3) allowed the more detailed observation that trait C (strongly reduced endosperm) resulted in 36% of abnormal seedlings but 37% of worst outcomes (dead and ungerminated). Even if van der Burg et al. (1994) described as abnormal an embryo with one or both cotyledons curved sideways, our outcome was that trait D (cotyledons curved sideways) produced also 40% of normal seedlings.

Moreover, van der Burg (1994) described one or both cotyledons sharply reflexed inside the seed as a cotyledon configuration producing abnormal seedlings, but we observed that the 74% of the seeds with trait E (reflexed cotyledons) produced normal seedlings.

Both traits F and G (small holes in the endosperm, fractures in the cotyledon(s)) actually do not represent important structural damage to the seeds, and the worst germination outcomes for F were due to the contemporary presence of A and D traits, which did not occur for G. This latter observation can be seen by looking at the full contingency table in the Supplementary Material S2, which reports all the combinations of morphological traits identified in each analysed seed.

3.2.2. *Quantitative morphology*

3.2.2.1. *Univariate analysis*. The image analysis of single seeds allowed different three-dimensional morphometric parameters, which quantitatively describe the internal and external seed structure, to be determined. The obtained mean values for each germination outcome after the final count (at 14 days), the standard errors and the significance of their differences are reported in Table 4. Parameters which refer to seed internal structure or external shape have been grouped as A and B, respectively.

Notwithstanding that our seed sample underwent a regular disinfection procedure and was exposed to X-rays for the microCT scans, 6 seeds out of 105 resulted as dead. Regarding such an outcome, it can be noted that there is no morphometric parameter able to differentiate the dead seeds from those having other germination outcomes (Table 4). This finding confirms that such a germination outcome has no relationship with external or internal seed morphometry. For

Table 3 – Predictive potential of qualitative morphological traits with respect to germination results at final count (14 d). Count of seeds with a given morphological trait arranged by germination outcome and their percentage with respect to the total of seeds with that trait.

	Morphological traits							
	A[a]	B[a]	C[a]	D[a]	E[a]	F[a]	G[a]	N
normal	0	0	6	2	23	38	22	22
abnormal	0	4	8	2	4	4	1	0
dead	1	0	3	1	2	2	0	2
ungerminated	2	2	5	0	2	1	0	0
Total	3	6	22	5	31	45	23	24
normal	0%	0%	27%	40%	74%	84%	96%	92%
abnormal	0%	67%	36%	40%	13%	9%	4%	0%
dead	33%	0%	14%	20%	6%	4%	0%	8%
ungerminated	67%	33%	23%	0%	6%	2%	0%	0%
Total	100%	100%	100%	100%	100%	100%	100%	100%

[a] Morphological traits that can be present both alone and with others in the analysed seeds.

Table 4 – Mean values of morphometric parameters for the expected outcomes (standard errors are reported in brackets). Means sharing a letter on a row are not statistically different (Tukey test) at a $P < 0.05$.

		Normal	Abnormal	Dead	Ungerminated
A	Free space %	6.02 (0.38)b	12.83 (1.56)a	11.30 (3.20)ab	14.64 (3.64)a
	Sauter diameter (mm)	0.66 (0.01)a	0.53 (0.04)b	0.54 (0.05)ab	0.48 (0.03)b
	Solid phase volume (mm^3)	2.30 (0.03)a	2.51 (0.05)a	2.23 (0.16)ab	1.89 (0.16)b
	Structure thickness (mm)	0.35 (0.00)a	0.30 (0.01)ab	0.29 (0.02)ab	0.26 (0.01)b
	Seed surface (mm^2)	21.38 (0.50)b	29.24 (1.57)a	26.00 (3.38)ab	23.63 (2.14)ab
	Equivalent rod length (mm)	25.92 (1.05)b	37.32 (3.50)a	37.04 (7.05)ab	36.04 (5.16)ab
	Structure model index	−3.62 (0.17)	−2.71 (0.29)	−3.13 (0.51)	−2.19 (0.51)
B	Major diameter (mm)	2.82 (0.02)b	3.04 (0.08)a	2.96 (0.12)ab	2.74 (0.08)b
	Total volume (mm^3)	2.45 (0.03)b	2.89 (0.06)a	2.54 (0.22)ab	2.24 (0.22)b
	Volume-equivalent sphere diameter (mm)	1.67 (0.00)b	1.76 (0.01)a	1.68 (0.04)ab	1.61 (0.05)b
	Sphericity	0.72 (0.00)ab	0.73 (0.00)a	0.70 (0.03)ab	0.68 (0.02)b
	Surface-equivalent sphere diameter (mm)	1.96 (0.00)	2.05 (0.01)	2.01 (0.04)	1.94 (0.04)
	Surface convexity index (1/mm)	−5.26 (0.22)	−6.88 (0.36)	−7.09 (0.62)	−4.46 (0.88)

A Internal structure dependent parameters.
B External shape dependent parameters.

this reason, we did not consider, in what follows, dead seeds as a germination outcome to be predicted.

Another general result is that the parameters of the A group discriminate better among the germination outcomes than the B group parameters. In particular, the free space % and Sauter diameter are able to significantly differentiate normal seeds from both abnormal and ungerminated seeds, with values respectively higher and lower than the normal seeds. Solid phase volume and structure thickness allowed normal seeds to be discriminated from ungerminated seeds.

Among the other A group parameters, seed surface and equivalent rod length allowed significant differentiation of normal from abnormal seeds, but did not distinguish from ungerminated seeds. This same reduced discrimination capacity has been exhibited by total volume, major diameter and volume equivalent sphere diameter of the B group. No discrimination capacity was observed for the other parameters of this group.

The significant increase (more than double the average) of free space % observed in abnormal and ungerminated seeds with respect to normal seeds agrees with the results reported in previous works that used X-ray radiography for different plant species. For bell pepper, Gagliardi and Marcos-Filho (2011) observed that seeds in which the area of the internal cavity occupied by the embryo and endosperm varied from 50 to 75% produced abnormal seedlings or did not germinate. Dell'Aquila (2007) found that when the seeds had open areas larger than 2.7% in most cases showed abnormal seedlings. Fernandes et al. (2016) verified that all lots of *Physalis peruviana* L. presented a progressive increase in the percentage of normal seedlings when the free area was smaller. Similar results have also been obtained with another plant of family Solanaceae, the aubergine, in the work of Silva et al. (2012). In the study by Gomes et al. (2019), who analysed selected microCT slices, for up to 10% of maize seed damaged area, seedling length and biomass decreased drastically. In our case, free space % was about 6% on average for normal seeds, and ranged between 12.8% and 14.6% for negative germination outcomes. Finally, Borges et al. (2019) showed that the average free area for tomato seeds that produced normal seedlings was 20%. Differences we found with respect to these cited works could be due to the different plant species or varieties considered, but may also reflect the coarser approximation in the determination of the parameter by means of two-dimensional radiography compared to our three-dimensional microtomography.

Even if, from a statistical point of view, Sauter diameter showed the same discriminant capacity as free space %, this latter exhibited larger relative difference in obtained values between normal and negative germination results, thus showing a larger sensitivity.

Regarding the tomato seed mass and external parameters, Peñaloza and Durán (2015) found that there is minor association with the subsequent seedlings, making it impossible to propose such measurements as a complement to quality evaluation tests. In our case, average seed mass showed significant differences only between abnormal and ungerminated seeds, being greater for the abnormal case (see Supplementary Material S3). Moreover, among the external parameters, major diameter, total volume and volume-equivalent sphere diameter showed average values significantly greater in abnormal than other germination outcomes. Overall, in our case larger seeds were the most related to abnormal seedlings.

The analysis of discriminant capacity of each single morphometric parameter with respect to the different germination outcomes is shown in Table 4.

3.2.2.2. *Multivariate analysis*. In order to evaluate the prediction potential of the whole set of morphometric parameters, a multivariate approach has been taken by means of discriminant analysis (DA). DA is a parametric method, which provides the group membership probability without the need for cross validation (Tharwat, 2016). A preliminary step to identify linearly correlated parameters by means of the Pearson correlation matrix is reported in Table 5, aiming to limit the multivariate analysis only to discriminant and independent variables. Therefore, only the morphometric parameters which allowed significant discrimination of at least two germination outcomes (see Table 4) were first included in the Pearson correlation matrix. Then, within the matrix in Table 5, we excluded the morphometric parameters that were strongly linearly correlated to others (i.e. with Pearson correlation coefficient larger

Table 5 – Pearson correlation coefficients (p-values below) among the morphometric traits.

	Sauter diameter	Solid volume	Structure thickness	Seed surface	Equivalent rod length	Major diameter	Seed volume	Vol eq sphere diameter	Sphericity
Free space %	-0.825[a]	-0.052	-0.730[a]	0.791[a]	0.815[a]	-0.038	0.354[a]	0.342[a]	0.404[a]
	0.000	0.597	0.000	0.000	0.000	0.701	0.000	0.000	0.000
Sauter diameter		0.155	**0.930**[a]	-.0772[a]	-0.816[a]	0.152	-0.175	-0.164	-0.307[a]
		0.113	0.000	0.000	0.000	0.122	0.074	0.094	0.001
Solid volume			0.069	0.450[a]	0.243[b]	0.624[a]	**0.914**[a]	**0.916**[a]	0.357[a]
			0.487	0.000	0.012	0.000	0.000	0.000	0.000
Structure thickness				-0.736[a]	-0.857[a]	0.122	-0.215[b]	-0.206[b]	-0.321[a]
				0.000	0.000	0.214	0.028	0.035	0.001
Seed surface					**0.919**[a]	0.244[b]	0.738[a]	0.728[a]	0.516[a]
					0.000	0.012	0.000	0.000	0.000
Equivalent rod length						0.073	0.553[a]	0.543[a]	0.475[a]
						0.457	0.000	0.000	0.000
Major diameter							0.562[a]	0.566[a]	-00.199[b]
							0.000	0.000	0.042
Seed volume								**0.997**[a]	0.503[a]
								0.000	0.000
Vol eq sphere diameter									0.505[a]
									0.000

Bold are indicated as the Pearson correlation coefficients larger than 0.9.
[a] Significant correlation at 0.01.
[b] Significant correlation at 0.05.

than 0.9 and with p-value <0.01) and, between two morphometric parameters that were strongly linearly correlated, we excluded the one with less discrimination capacity. In particular, between Sauter diameter and structure thickness, the latter was excluded because of its lower discrimination capacity than Sauter diameter, whose average value for normal seeds was significantly different from both those of abnormal and ungerminated seeds. Also, among solid phase volume, seed volume and volume equivalent sphere diameter, the latter two were excluded because of their lower discrimination capacity. Among seed surface and equivalent rod length, which showed the same discrimination capacity, the latter was excluded because of its less intuitive definition. In the loadings plot in Fig. 3b the morphometric parameters used for the DA regarding the germination outcomes at final count are reported. It can be noted that all are internal morphometric parameters (A group), except for sphericity (B group).

In the case of the final count, using DA to predict the membership of seeds in three groups (normal, abnormal, ungerminated), the two discriminant functions DF1 and DF2 in Fig. 3 explain 100% of the variability of the morphometric parameters. In Fig. 3b it can be seen that free space % and Sauter diameter were the better correlated with DF1, which explains 64.6% of the variability, while the other parameters were better correlated with DF2. Such a result confirms the overall univariate analysis, where free space % and Sauter diameter have been recognised as the most discriminant morphometric parameters.

Figure 3a shows the score plot from DA. The group membership prediction regions shown are those obtained in the case of common covariance matrix. The position of the group centroids allows the distance of the normal centroid from the ungerminated to be shown to have a larger projection on the DF1 axis, which means that such seed groups are different mainly for the morphometric parameters better correlated with DF1, that is free space % and Sauter diameter. The position of the abnormal centroid suggests that seeds of that group can be differentiated from those of the other two groups on average for all the parameters together. In Fig. 3a, it can also be noted that normal* scores lie almost completely in the normal membership prediction region and such a result confirms correctness of the hypotheses made in Appendix A to identify seeds whose germination outcome was affected by exposure to X-rays. A further confirmation that, except for the X-ray exposure effects, normal and normal* seed groups are homogeneous comes from the observation that the percentage of seeds that had germinated by the first count was about the same in normal and normal* groups (50.8% and 47.8%, respectively), while for abnormal group such percentage was 27.3% and 33.3% for dead seeds (data provided in third column of the table in Supplementary Material S5).

DA based on morphometric parameters allowed, overall, the prediction of 91.9% and 90.9% of germination outcomes in case of common and separate within-group covariance matrices, respectively. In Table 6 the classification results as both occurrence and percentage are reported. It can be noted in particular that the best prediction potential (96.3% or 95.1%, depending on covariance matrix assumptions) was for the normal germination outcome, followed by ungerminated (83.3%) and abnormal (63.6%). Such results show that the three-dimensional morphometric characterisation of internal structure of tomato seeds has a very good potential to predict germination outcomes. The least easy to predict result was the abnormal germination outcome and this is then the least related to seed morphology. Complete DA results are reported in the Supplementary Material S4.

Overall, among all the analysis approaches used in this work to investigate the relationship between seed morphology and tomato seed germination, DA proved the most accurate and powerful. A similar outcome was found by de Medeiros

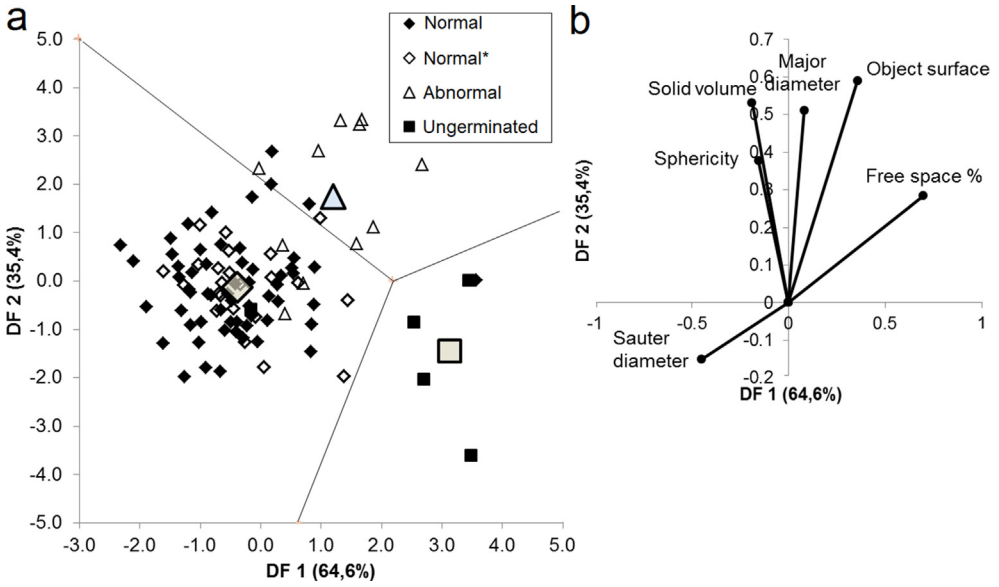

Fig. 3 – Discriminant analysis. a) Score plot with the group centroids and group membership regions (case of linear separation boundaries). Groups are germination outcomes. Normal* tagged scores refer to seeds affected by X-rays exposure. b) Loadings plot.

Table 6 – Classification results from DA. In brackets are results in case of quadratic separation boundaries.

Germination outcome		Predicted group membership			Original
		Ungerminated	Abnormal	Normal	
Count	Ungerminated	5	0	1	6
	Abnormal	0	7	4	11
	Normal	1	2 (3)	79 (78)	82
%	Ungerminated	83.3	0.0	16.7	100
	Abnormal	0.0	63.6	36.4	100
	Normal	1.2	2.4 (3.7)	96.3 (95.1)	100

91.9% (90.9%) of original grouped cases correctly classified.

et al. (2020), who studied germination of *Jatropha curcas* seeds by means of DA of morpho–densitometric parameters, obtained from two-dimensional radiographic images.

4. Conclusions

Use of X-ray micro-CT for imaging of tomato seeds has proved to be effective for studying the relationship between seed morphology and germination. Indeed, the morphometric parameters we found most useful for that purpose were those taking into account the internal structure of the seeds. The only external shape parameter that gave a minor contribution was sphericity.

Our experimental results confirm that, in this order, abnormalities of the whole embryo, defects in endosperm, and defects in cotyledons showed a decreasing negative impact on germination. This refers to the counts of germination outcomes after both 5 and 14 days.

A large number of morphometric parameters describing internal structure of the seeds can be calculated by means of image analysis but we observed that a preliminary check of their mutual correlations is advisable to enhance the successive multivariate analyses. As single parameters, the three-dimensional free space % and Sauter diameter have proved to be the most diagnostic for germination outcomes, while the discriminant analysis on the whole dataset of uncorrelated morphometric parameters allowed a very high percentage of success in prediction of germination outcome, overall. In particular, the correct prediction of seed group membership was highest for normal seedlings, followed by ungerminated seeds, and abnormal seedlings. The latter germination outcome was more frequent in larger sized seeds.

In our study, for the first time, three-dimensional morphological traits of tomato seeds have been scored in great detail and have been singularly associated with the corresponding germination outcome. Thus we have obtained an experimental confirmation of the different importance of the seed components for germination. To the best of our knowledge, our work is also the first example of the application of DA to three-dimensional morphometric parameters of tomato seeds to predict germination outcomes, and such an approach proved the most powerful among all the performed analyses.

Overall our work confirms the usefulness of X-rays to obtain promising results on the relationship between seed morphology and physiological quality. However, the experiments we carried out showed also that the level of X-ray exposure due to microtomographic scans can have a negative impact on tomato seed germination, with a significant increase in the number of abnormal seedlings. This, therefore, suggests a need to carefully address the use of X-ray micro-CT if aiming to develop industrial systems for tomato seed testing or sorting.

Declaration of competing interest

The authors declare that they have no known competing financial interests or personal relationships that could have appeared to influence the work reported in this paper.

Appendix A. Procedure for identification of seeds whose germination result was affected by X-ray exposure

From X-ray absorption experiment the following relationship was found:

abnormal ratio = 0.0970 + (0.651 * Level of X-ray radiation)

This means that in a germination test, we would expect 9.7% of abnormal seedlings without X-ray exposure. For the seed lot used in the morphology experiment with 105 units, we should expect 105*0.097 = 10.185 abnormal seedlings, i.e. 11 rounded to the superior integer.

Thus, because we obtained 34 abnormal seedlings, we hypothesised that in our experiment 23 seeds provided abnormal seedlings due to X-ray exposure, which otherwise would have resulted in normal seedlings.

As normal seedlings were gradually less frequent in the seeds showing N, G, F and E traits (see the histogram in Figure A1), we selected the seeds to be considered normally sprouted choosing, among the 34 abnormal seeds, first those having trait N, then G, F and E, till reaching the number of 23 seeds. Such 23 seeds are tagged as normal* in the Supplementary Material S5.

According to this criterion, except for Fig. 2, in the results throughout the paper we considered the seeds with IDs 2, 7, 14, 17, 25, 26, 30, 46, 55, 56, 57, 6, 64, 65, 69, 70, 72, 73, 74, 79, 80, 87, 99 as cases which provided normal seedlings. However, we tracked such reclassified seeds by tagging them as normal*, in order to be able to evaluate the consequences of our choice.

It should be noted that no seeds among the 23 have been reclassified as ungerminated or dead because the results in Fig. 2 showed that the X-ray exposure didn't affect the frequency of ungerminated and dead seeds.

Appendix B. Intermediate results at first count (5days)

For the first count (at 5 days) it was possible to score only the germinated or ungerminated seeds, since after 5 days from sowing not all seeds have germinated and seedlings are at the very beginning of their development. The germinated seeds were 46, corresponding to 43.8% of all the seeds. Among the germinated seeds, 89.1% provided normal seedlings, 6.5% abnormal seedlings and 4.3% dead seeds at the final count.

Table B1 shows that the percentage of germinated seeds increased according to the alphabetical order of the traits, except for A and G traits. However, the germinated seed with trait A was dead at 14 days, as it can be noted from the whole dataset record (Supplementary Material S5). Such a result confirms what was observed for the final count, i.e. the alphabetical order chosen to define the morphological traits corresponds overall to decreasing negative effects on seed germination.

Among the morphometric parameters (Table B2), only free space % and seed surface showed significant difference between germinated and ungerminated seeds. A certain correlation between free area and first count results has also been found by Borges et al. (2019) for tomato seeds.

DA has been performed applying the same procedure used for the final count results, and the morphometric parameters used were again free space % and seed surface. Classification results are reported in Table B3. Only 59.0% of original grouped cases were correctly classified and the prediction of germinated seeds (45.7%) was more difficult than for ungerminated seeds (69.5%). Thus, the morphometric traits exhibit a lower prediction potential for the germination at first count than at final count. Such a result can be due to the fact that the first count after 5 days is at too early a development stage of the sprouts to understand what will be the final germination outcome, at least for the tomato variety used in this work.

Appendix C. Supplementary data

Supplementary data to this article can be found online at https://doi.org/10.1016/j.biosystemseng.2020.09.003.

REFERENCES

Ahmed, M. R., Yasmin, J., Collins, W., & Cho, B. K. (2018). X-ray CT image analysis for morphology of muskmelon seed in relation to germination. *Biosystems Engineering, 175*, 183–193.

Arkhipov, M. V., Priyatkin, N. S., Gusakova, L. P., Potrakhov, N. N., Gryaznov, A. Y., Bessonov, V. B., Obodovskii, A. V., & Staroverov, N. E. (2019). X-ray computer methods for studying the structural integrity of seeds and their importance in modern seed science. *Technical Physics, 64*(4), 582–592.

Bino, R. J., Aartse, J. W., & Van Der Burg, W. J. (1993). Non-destructive X-ray analysis of Arabidopsis embryo mutants. *Seed Science Research, 3*(3), 167–170.

Blaschke, T. (2010). Object based image analysis for remote sensing. *ISPRS Journal of Photogrammetry and Remote Sensing, 65*(1), 2–16.

Borges, S. R. D. S., Silva, P. P. D., Araújo, F. S., Souza, F. F. D. J., & Nascimento, W. M. (2019). Tomato seed image analysis during the maturation. *Journal of Seed Science, 41*(1), 22–31.

Dell'Aquila, A. (2007). Towards new computer imaging techniques applied to seed quality testing and sorting. *Seed Science & Technology, 35*(3), 519–538.

de Medeiros, A. D., Zavala-León, M. J., da Silva, L. J., Oliveira, A. M. S., & Dias, D. C. F. D. S. (2020). Relationship

between internal morphology and physiological quality of pepper seeds during fruit maturation and storage. *Agronomy Journal, 112*, 25–35.
Dhamgaye, S., Dhamgaye, V., & Gadre, R. (2018). Growth retardation at different stages of bean seedlings developed from seeds exposed to synchrotron X-ray beam. *Advances in Biological Chemistry, 8*, 29–35.
Downie, B., Gurusinghe, S., & Bradford, K. J. (1999). Internal anatomy of individual tomato seeds: Relationship to abscisic acid and germination physiology. *Seed Science Research, 9*(2), 117–128.
Fernandes, J. S., da Silva, D. F., dos Santos, H. O., & Pinho, É. D. R. (2016). X-ray test in the evaluation of quality seed of physalis at different stages of development. *Revista de Ciências Agroveterinárias, 15*(2), 165–168.
Gagliardi, B., & Marcos-Filho, J. (2011). Relationship between germination and bell pepper seed structure assessed by the x-ray test. *Scientia Agricola, 68*, 411–416.
Gargiulo, L., Grimberg, Å., Repo-Carrasco-Valencia, R., Carlsson, A. S., & Mele, G. (2019). Morpho-densitometric traits for quinoa (*Chenopodium quinoa* Willd.) seed phenotyping by two X-ray micro-CT scanning approaches. *Journal of Cereal Science, 90*, 102829.
Gomes, F. G., jr., Cicero, S. M., Vaz, C. M. P., & Lasso, P. R. O. (2019). X-ray microtomography in comparison to radiographic analysis of mechanically damaged maize seeds and its effect on seed germination. *Acta Scientiarum. Agronomy, 41*, Article e42608.
Gomes, F. G., jr., & van Duijn, B. (2017). Three-dimensional (3- D) X-ray imaging for seed analysis. *Seed Testing International, 154*, 48–52.
Hildebrand, T. O. R., & Rüegsegger, P. (1997). Quantification of bone microarchitecture with the structure model index. *Computer Methods in Biomechanics and Biomedical Engineering, 1*(1), 15–23.
International Seed Testing Association. (2019). *International rules for seed testing*. Seed Science & Technology. https://doi.org/10.15258/istarules.2019. i–19-8 (300).
Peñaloza, P., & Durán, J. M. (2015). Association between biometric characteristics of tomato seeds and seedling growth and development. *Electronic Journal of Biotechnology, 18*(4), 267–272.
Porsch, F. (2020). Automated seed testing by 3D X-ray computed tomography. *Seed Science & Technology, 48*(1), 73–81.
Rezk, A. A., Al-Khayri, J. M., Al-Bahrany, A. M., El-Beltagi, H. S., & Mohamed, H. I. (2019). X-ray irradiation changes germination and biochemical analysis of two genotypes of okra (Hibiscus esculentus L.). *Journal of Radiation Research and Applied Sciences, 12*(1), 393–402.
Silva, V. N., Cicero, S. M., & Bennett, M. (2012). Relationship between eggplant seed morphology and germination. *Revista Brasileira de Sementes, 34*(4), 597–604.
Silva, V. N., Cicero, S. M., & Bennett, M. (2013). Associations between X-ray visualised internal tomato seed morphology and germination. *Seed Science & Technology, 41*(2), 225–234.
Tharwat, A. (2016). Linear vs. quadratic discriminant analysis classifier: A tutorial. *International Journal of Applied Pattern Recognition, 3*(2), 145–180.
Van der Burg, W. J., Aartse, J. W., Van Zwol, R. A., Jalink, H., & Bino, R. J. (1994). Predicting tomato seedling morphology by X-ray analysis of seeds. *Journal of the American Society for Horticultural Science, 119*(2), 258–263.
Xia, Y., Xu, Y., Li, J., Zhang, C., & Fan, S. (2019). Recent advances in emerging techniques for non-destructive detection of seed viability: A review. *Artificial Intelligence in Agriculture, 1*, 35–47.